

Oxidation of aluminum and relevant polarization in dc biased silver metaphosphate glass

A. DOI

Department of Materials, Nagoya Institute of Technology, Nagoya 466-8555, Japan
E-mail: akiradoi@mse.nitech.ac.jp

A comprehensive study was made on biasing the silver metaphosphate glass with a dc pulse train, by using sputtered aluminum or evaporated aluminum as the anode. Oxidation of aluminum proceeded at the anode-glass interface, and relevant polarization and depolarization peaks were seen at the onsets of biasing and off biasing, respectively. It was suggested tentatively that the polarization arose from orientational motion of the P–O dipoles within the oxide, with 54 ± 1 kJ/mol as the activation energy for relaxation.

© 2003 Kluwer Academic Publishers

1. Introduction

When we want to study ion dynamics in ion-conducting glass electrically, we usually deposit metal electrodes on both sides of a sample, bias it with dc/ac voltage, and measure the electrical response via the electrodes. Therefore, the observed response must inevitably be electrode-related. The present author has long used gold and silver as the electrodes [1]. As is well known, gold acts virtually as a blocking anode (from which no injection of the anode metal ions is possible) while silver is very easily injected into glass when it is used as the anode.

Recently, a preliminary study was made on dc biasing the silver metaphosphate (AgPO_3) glass using evaporated aluminum as the anode metal [2]. Aluminum has stronger affinity for oxidation than gold and silver. Therefore, we expect that oxidation of aluminum (the so-called “anodization”) would proceed if aluminum is used in lieu of gold and silver as the anode. The AgPO_3 glass is a silver-ion conductor. However, the studies with an X-ray photoelectron spectroscopy (XPS) suggest that the metaphosphate (PO_3^-) ions would conduct toward the anode besides the silver ions conducting toward the cathode [2, 3]. As a result, dc biasing the aluminum-anoded glass generated a dielectric oxide at the anode-glass interface, possibly by electrochemical reaction of the PO_3^- ions with the aluminum anode. The purpose of the present study was to gain further insight into the nature of solid-state anodization of aluminum on the silver metaphosphate glass, by using sputtered aluminum or evaporated aluminum as the anode.

2. Experimental

The samples were made by melting a mixture of appropriate amounts of AgNO_3 and $\text{NH}_4\text{H}_2\text{PO}_4$ in a platinum crucible at 500°C for 1–2 h, quenching on a carbon plate to a thickness of ~ 0.6 mm, and depositing aluminum (300–500 Å thick) and gold (~ 400 Å thick) on both sides. The resulting samples, in the configura-

tion $\text{Al}/\text{AgPO}_3/\text{Au}$, were labeled *E* or *S* according to whether the aluminum anode was made by evaporation (*E*) or by dc sputtering using argon ions (*S*).

A sample was biased with a pulse train, made of pulses of height V_i and width 50 ms followed by 50 ms of off-voltage, and the induced current, i , was detected as an output voltage, $V_o (= iR_r)$, across a reference resistor $R_r (= 1.18 \Omega)$ by an oscilloscope. The applied field for forming an oxide layer (termed the “forming field”), E_{i0} , was varied from 10 to 750 V/cm. The measurements were made in vacuo ($\sim 10^{-6}$ torr), at or below 140°C which is about twenty degrees below the glass transition temperature [4].

After dc biasing, the depth profiles of Al, Ag, P, and O were measured from the anode surface by XPS after intermittent etchings of the surface by an argon-ion beam. Since the etching rate was different for different compositions and materials as well as variable experimental settings, the sputtering time rather than the depth was used as the abscissa.

3. Results

Figs 1 and 2 compare the depth profiles of virgin (i.e., non-biased) samples E-I and S-I, and the ratios of number of atoms for oxygen-to-phosphorus, O/P, and silver-to-phosphorus, Ag/P, as a function of the sputtering time. The depths at the ends of the sputtering time were $0.1 \mu\text{m}$. The near parallelism in the depth profiles of oxygen and phosphorus (except excess accumulation of oxygen at the anode-glass interface) suggests preferential movement of the negative ions in the form of PO_3^- toward the anode during deposition of aluminum [3]. The rise of oxygen concentration at the outermost surface is due to a “passive” film, formed on exposure of as-deposited aluminum to the air. For sample E-I, we see the peaks of oxygen and phosphorus concentrations below the anode, followed by their troughs where silver in alternation gave the peak. Such undulations are not seen for sample S-I.

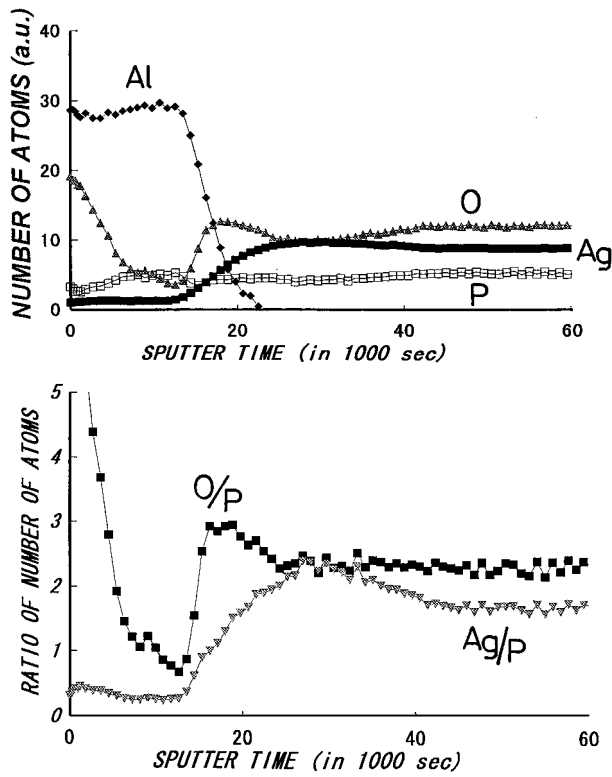


Figure 1 Depth profiles of virgin sample E-I and the ratios of number of atoms for oxygen-to-phosphorus, O/P, and silver-to-phosphorus, Ag/P, thereof.

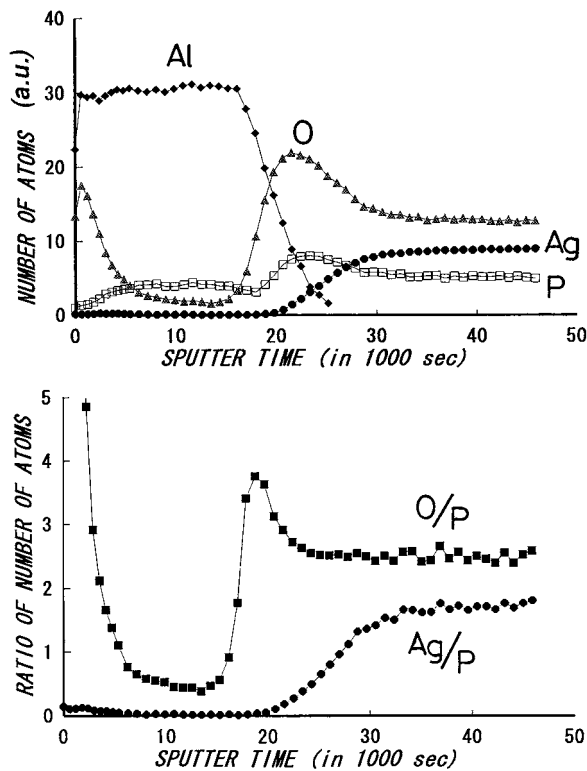


Figure 2 Depth profiles of virgin sample S-I and the ratios of number of atoms for O/P and Ag/P thereof.

Although there are some differences in the depth profiles of virgin-E and -S samples, the depth profiles after dc biasings resembled to each other and were similar to Fig. 10 in [2]. Besides, no differences in the electrical responses to dc biasings were found between E and S samples either. For example, Fig. 3 shows the

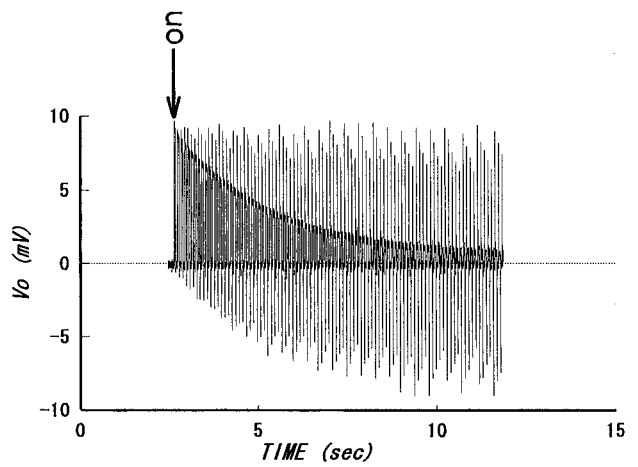


Figure 3 Electrical response of sample S-II to 500 V/cm biasing with a pulse train at 96°C.

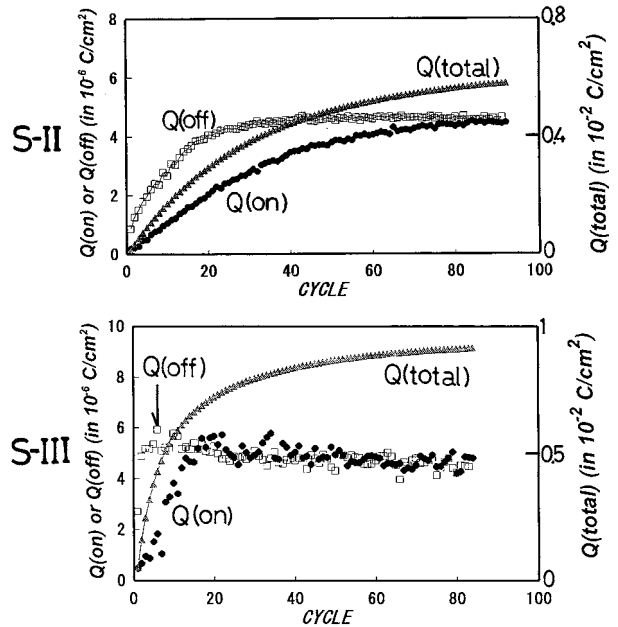


Figure 4 Cycle-dependencies of $Q(\text{on})$, $Q(\text{off})$, and $Q(\text{total})$ for sample S-II at 96°C and sample S-III at 140°C, both to 500 V/cm biasings.

response curve of sample S-II to 500 V/cm biasing at 96°C. In addition to the conduction current which decayed monotonously to zero, with the overall charge of 0.0068 C/cm², the sharp positive and negative current peaks were seen at the onsets of biasing and off biasing, respectively. Periodic undulations in the peak heights are the “beats,” caused by mismatch of our slow (40 kS/s) sampling rate with the fast relaxational process.

Sample S-III was biased with 500 V/cm at 140°C. The electrical response of this sample was almost identical with the reported one [2], with 0.0091 C/cm² as the overall charge flowed. Fig. 4 shows the areas covered by the sharp peaks during biasing, $Q(\text{on})$, and during off biasing, $Q(\text{off})$, as well as the total conduction charge flowed on biasing up to a given cycle, $Q(\text{total})$, for samples S-II and S-III. The ratio $Q(\text{on})/Q(\text{total})$ was plotted for both samples, as well as for sample E-II for which biasing was made at 140°C with 500 V/cm (Fig. 5).

The formation or annihilation process of polarization on biasing or on off biasing is given by the charging or

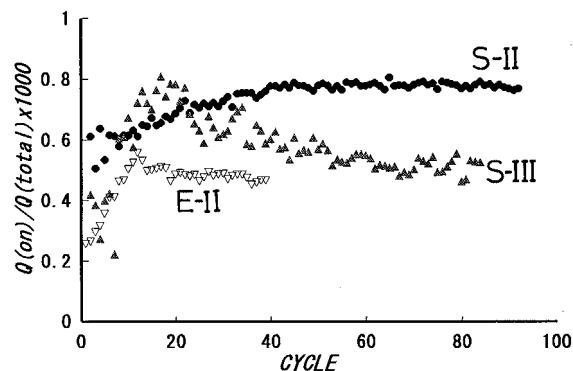


Figure 5 Cycle-dependencies of the ratio $Q(\text{on})/Q(\text{total})$ for sample S-II at 96°C, sample S-III at 140°C, and sample E-II at 140°C, all to 500 V/cm biasings.

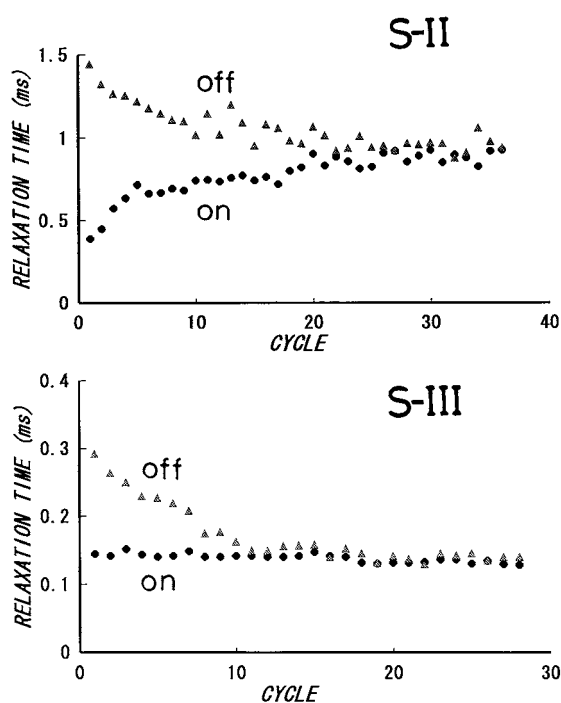


Figure 6 The relaxation time of polarization for sample S-II to 500 V/cm biasing at 96°C and sample S-III to 500 V/cm biasing at 140°C, as estimated from the polarization/depolarization peaks on biasing ("on") and on off biasing ("off").

discharging current of the form

$$i = i_0 \exp(-t/\tau) \quad (1)$$

provided the relaxation time, τ , is single-valued. Fig. 6 shows the estimated τ values from the initial slopes of the $\log i$ versus t curves for samples S-II and S-III. It is to be noted that τ in reality has some distribution, those shown in Fig. 6 being the initial but dominant values.

In our glass, the silver ions are the dominant charge carriers. When this glass is biased with a pulse train, especially when gold is used as the anode, the silver ions conduct first, leaving the positive-ion depleted region (PDR) underneath the anode. On off biasing, some of the silver ions which conducted in the last cycle of biasing back-diffused into the PDR and gave the negative current [3]. Even in our aluminum-anoded samples, the silver ions would conduct toward the cathode and generate the PDR. On off biasing, back-diffusion of

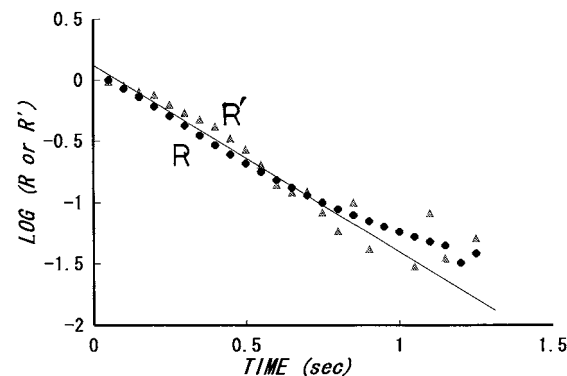
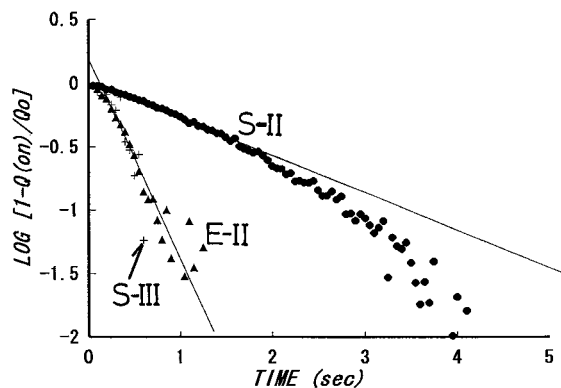


Figure 7 Logarithmic plots of $[1 - Q(\text{on})/Q_0]$ as a function of biasing time for sample S-II to 500 V/cm biasing at 96°C, and for samples S-III and E-II to 500 V/cm biasings at 140°C, respectively. (Bottom) Logarithmic plots of R (the ratio of the conduction charge in a given cycle of biasing to the conduction charge in the initial cycle of biasing) and of $R' (= 1 - Q(\text{on})/Q_0)$ for sample E-II.

the silver ions would induce the negative current too, besides the negative current by annihilation of polarization. This may be the reason for larger values of $Q(\text{off})$ and $\tau(\text{off})$ as compared to $Q(\text{on})$ and $\tau(\text{on})$ (Figs 4 and 6).

With increasing cycles, however, $Q(\text{off})$ and $\tau(\text{off})$ approached $Q(\text{on})$ and $\tau(\text{on})$, respectively. The growth of $Q(\text{on})$ with cycles may reflect the growth of the oxide, so is given in the form

$$Q(\text{on}) = Q_0[1 - \exp(-t/\tau(\text{ox}))], \quad (2)$$

where $\tau(\text{ox})$ is the relaxation time for oxidation which characterizes the process of oxidation. The initial slopes of $\log [1 - Q(\text{on})/Q_0]$ versus t gave 0.3 s for $\tau(\text{ox})$ of samples S-III and E-II at 140°C, while 1.5 s for sample S-II at 96°C (Fig. 7). These $\tau(\text{ox})$ values are in rough accord with those estimated from the conduction current curves. This is exemplified in the bottom of Fig. 7 for sample E-II, where the curves of $\log [R$ (the ratio of the conduction charge flowed in a given cycle of biasing to the conduction charge flowed in the initial cycle of biasing)] and $\log [R' (= 1 - Q(\text{on})/Q_0)]$ gave the same initial slopes. The Arrhenius plots of $\tau(\text{ox})$ gave about 46 kJ/mol as the activation energy for oxidation.

The saturated value of $Q(\text{on}) (= Q(\text{off}))$, Q_0 , was indifferent to the forming field (E_{i0}) applied, except below 100 V/cm (Fig. 8). From the relation

$$Q = CV, \quad (3)$$

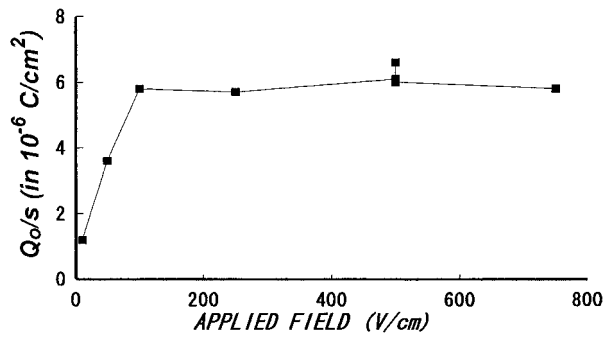


Figure 8 The saturated value of polarization, Q_0 , at 140°C as a function of the applied (forming) field, E_{i0} . The data are from *S* and *E* samples.

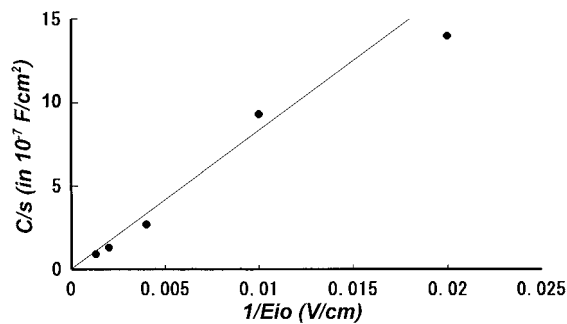
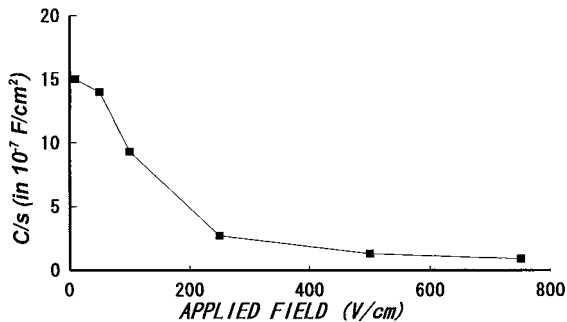


Figure 9 The capacitance, C , at 140°C as a function of the applied (forming) field, E_{i0} , or of $1/E_{i0}$. The data are from *S* and *E* samples.

the capacitance of our electrolytic capacitor, C , was calculated. It was found that C increased approximately linearly with a reciprocal of E_{i0} (Fig. 9). Similarly, τ_0 , the saturated value of $\tau(\text{on}) (= \tau(\text{off}))$, increased approximately linearly with $1/E_{i0}$ (Fig. 10). The curve of Fig. 9 is well understood on the ground that the thickness of the oxide attained, at end cycles of biasing, increases in proportion to the forming voltage, V_{i0} , or to the forming field (E_{i0}), if sample thicknesses are the same, more or less. The approximately linear growth of the oxide with V_{i0} is well known in the fabrication of an electrolytic capacitor in a liquid electrolyte. The departure from linearity below 100 V/cm (Figs 9 and 10) may reflect some incompleteness in the oxide formed, although biasing even with 10 V/cm at 140°C (for sample S-IV) yielded coincidences between $Q(\text{on})$ and $Q(\text{off})$ and between $\tau(\text{on})$ and $\tau(\text{off})$ at end cycles of a pulse train (not shown).

After biasing with E_{i0} of 100 V/cm at 140°C, sample S-V was cooled to lower temperatures stepwise and biasings were repeated. No more conduction currents were seen, except the sharp positive and negative peaks at the onsets of biasing/off biasing. This sequence

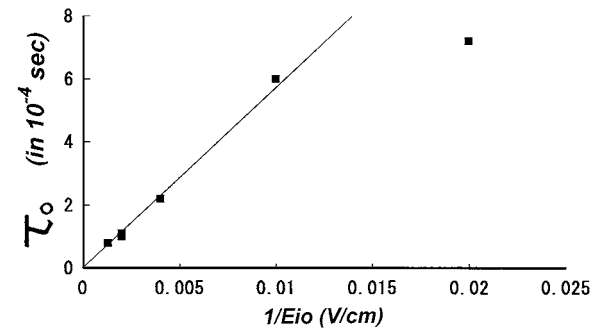
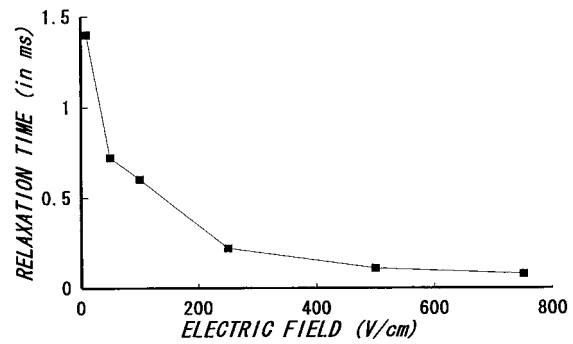


Figure 10 The relaxation time, τ_0 , at 140°C as a function of the applied (forming) field, E_{i0} , or of $1/E_{i0}$. The data are from *S* and *E* samples.

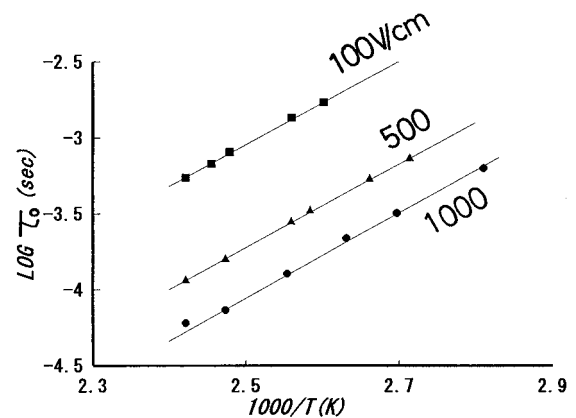


Figure 11 Arrhenius plots of the relaxation time, τ_0 , for sample S-V on initial biasing with 100 V/cm at 140°C, followed by biasings with 100 V/cm at several temperatures below 140°C. This sequence was repeated by biasing with 500 V/cm at 140°C, then by biasing with 1000 V/cm at 140°C.

was repeated by biasings with 500 V/cm, then with 1000 V/cm. It was found that τ_0 decreased irreversibly with an increase in E_{i0} , fitting into the curve of Fig. 10, although Q_0 was almost fixed. The Arrhenius plots of τ_0 (Fig. 11) reveal that the activation energy for relaxation is constant (54 ± 1 kJ/mol) irrespective of E_{i0} applied.

The capacitance of an electrolytic capacitor thus formed would remain intact, satisfying Equation 3, when the capacitor is biased with a voltage V_i which is less than the forming voltage, V_{i0} . Truly, C and τ were found to be approximately constant while Q_0 decreased with decreasing V_i for sample E-III when, after initial biasing with the forming field of 500 V/cm at 140°C, the sample was subjected to biasing again with 500 V/cm, followed by biasing with 200 V/cm, then with 100 V/cm (Table I). The Arrhenius behavior of τ_0 was reversible, unless biasing was made with a field higher than E_{i0} .

TABLE I List of $Q(\text{total})$, the total charge flowed during biasing till conduction-current cease; Q_o , the saturated value of polarization; C , the capacitance; and τ , the relaxation time, for sample E-III which, after initial biasing with 500 V/cm at 140°C, was biased again with 500 V/cm, followed by biasing with 200 V/cm, then with 100 V/cm

E_i (V/cm)	$Q(\text{total})$, C/cm ²	Q_o/s (C/cm ²)	C/s (F/cm ²)	(sec)
500 (initial)	0.0099	6.2×10^{-6}	1.2×10^{-7}	0.98×10^{-4}
500	—	5.5×10^{-6}	1.0×10^{-7}	1.0×10^{-4}
200	—	1.6×10^{-6}	0.73×10^{-7}	0.89×10^{-4}
100	—	0.83×10^{-6}	0.80×10^{-7}	0.78×10^{-4}

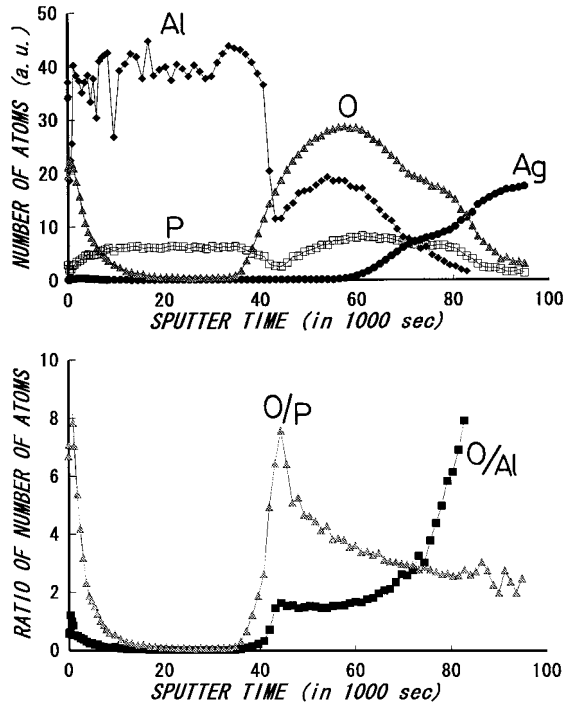


Figure 12 Depth profiles from the aluminum anode side of sample E-III after biasing with 500 V/cm at 140°C and the ratios of number of atoms for O/P and O/Al thereof. The depth at the end of the sputtering time was 0.06 μm .

The depth profiles were measured for many E and S samples, but the general features seen are similar to those reported [2], with the shoulder at its tail of the profile of aluminum and the corresponding peaks in oxygen and phosphorus, followed by the plateaus in oxygen, phosphorus, and silver. The initial peaks underneath the anode are assigned tentatively to the relevant oxide [2]. Only for one sample could we see the oxide which was isolated from the overlapping aluminum anode. Fig. 12 shows the depth profiles of sample E-III after biasing with 500 V/cm at 140°C. At the bottom are shown the ratios of number of atoms for O/P and O/Al. The ratio of O/Al at its plateau (near the sputtering time of 5×10^4 s) was about 1.5, suggesting that the composition of our oxide is $\text{Al}_2(\text{P}_x)\text{O}_3$, with $x < 1$. The thicknesses of the oxide layers were 10–20 nm. Silver seems not to be the main constituent of the oxide, since it appeared from underneath the oxide. We are uncertain whether the oxide is crystalline or non-crystalline, although X-ray diffraction studies gave no sign of a crystal. It is well known that the aluminum oxide formed by liquid-phase anodization is amorphous.

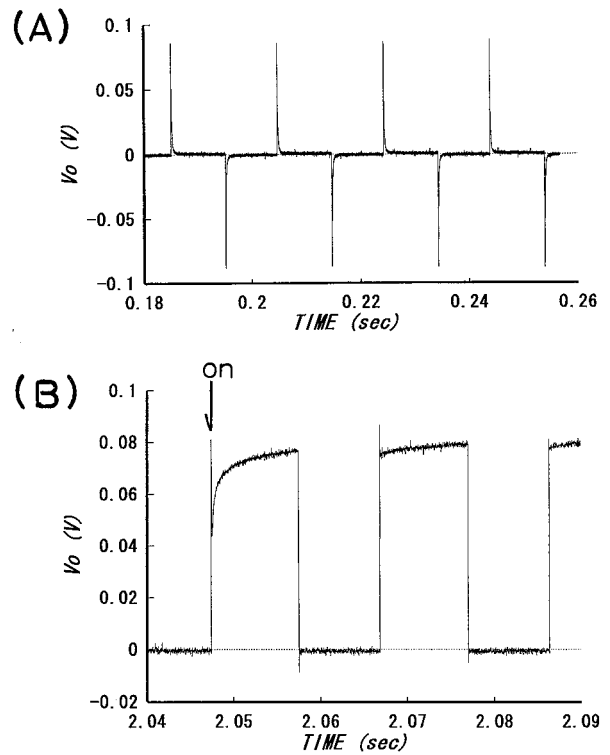


Figure 13 (A) Electrical response of aluminum-anodized sample S-VI to 500 V/cm biasing at 140°C, after biasing till conduction-current cease. (B) Initial response of this sample on reverse polarity, now with gold as the anode.

Finally, let us consider biasing sample S-VI with 500 V/cm at 140°C, firstly with aluminum as the anode till conduction-current cease; then the polarity was reversed, now with gold as the anode (Fig. 13). (In this case, the pulse train was made of pulses of 10 ms duration, followed by 10 ms of off biasing.) On reverse biasing, the sharp positive and negative peaks due to polarization/depolarization were annihilated within initial several cycles. This exemplifies the peculiar nature of an electrolytic capacitor that its function as a capacitor can easily be destroyed when it is biased in reverse polarity.

4. Discussion

At a given cycle of biasing and off biasing, the estimated charge $Q(\text{on})$ is the charge induced in the external circuit by the formation of polarization, by

$$Q(\text{on}) = C \Delta V, \quad (4)$$

where ΔV is a potential drop across the oxide. The capacitance, C , may be given by

$$C/s = \epsilon_o \epsilon(\text{ox})/d(\text{ox}), \quad (5)$$

where ϵ_o is the permittivity of free space and $\epsilon(\text{ox})$ is the relative dielectric function of the oxide.

Suppose $\epsilon(\text{ox})$ and the resistivity of the oxide are invariable in the course of anodization. At initial cycles of biasing, the oxide may be very incomplete in its morphology as a dielectric, perhaps be dappled, to give a small ΔV and small $Q(\text{on})$. With increasing cycles, however, the oxide would grow from a dappled

to a continuous or planar layer. Once the oxide becomes continuous (at which ΔV may still be less than V_{io}), $Q(\text{on})$ would remain constant ($= Q_o$) during further oxide growth, till saturation in $Q(\text{total})$ at which ΔV reaches V_{io} . This may be the reason why the ratio $Q(\text{on})/Q(\text{total})$ passed through the maximum (at 0.6–0.8 s) to a decline for 140°C-biased samples S-III and E-II (Fig. 5). (The difference between S-III and E-II is unknown at present.) For 96°C-biased sample S-II, on the other hand, it took far longer time before the ratio reached maximum. At final cycles, Equations 4 and 5 give

$$Q_o/s = \epsilon_o \epsilon(\text{ox}) V_{io}/d(\text{ox}). \quad (6)$$

Q_o/s must be fixed constant irrespective of V_{io} (or E_{io}) applied (Fig. 8), provided $d(\text{ox})$ increases linearly with V_{io} .

The dielectric function of crystalline alumina is almost frequency independent in the range of 10^2 – 10^{10} Hz [5]. This indicates the absence, in the genuine alumina, of the permanent dipoles as ours having the relaxation time as large as 10^{-4} s at 140°C. The XPS data implies that our oxide is of the composition $\text{Al}_2(\text{P}_x)\text{O}_3$, with $x < 1$. The depth profiles (Fig. 12) suggest variation in the concentration of the phosphorus atoms within the oxide, having smaller x in the very proximity of the anode. A hypothesis based on the data of τ_o (Figs 10 and 11 and Table I) is that the polarization arises from orientational motion of the P–O dipoles within the aluminum oxide, that the motion is retarded by the presence of the intervening silver ions, and that the amount of those silver ions is gradually and irreversibly removed out of the oxide with an increase in E_{io} .

5. Conclusion

A comprehensive study was made on biasing the silver metaphosphate glass with a dc pulse train, using sputtered aluminum or evaporated aluminum as the anode. No particular differences were found between them in

their electrical responses. The experiments suggest that the oxide formed at the anode–glass interface on biasing may be responsible for the observed dielectric behavior. The results are summarized as follows:

(1) The response curve of a sample to biasing with a dc pulse train can well be understood on the ground that the oxide was initially dappled, but grew to a continuous or planar layer when $Q(\text{on})$ reached saturation ($= Q_o$), till no further oxidation when a potential drop across the oxide layer reached the forming voltage. It is suggested from the E_{io} -dependences of Q_o and τ_o that the oxide thickness grows with E_{io} almost linearly, at least with E_{io} of more than 100 V/cm at 140°C. The activation energy for oxidation is about 46 kJ/mol.

(2) The composition of the oxide may be $\text{Al}_2(\text{P}_x)\text{O}_3$, with $x < 1$. It is suggested that the polarization arises from orientational motion of the P–O dipoles within the aluminum oxide, that the motion is retarded by the presence of the intervening silver ions, and that the amount of those silver ions is gradually and irreversibly removed out of the oxide with an increase in E_{io} . The activation energy for relaxation was 54 ± 1 kJ/mol irrespective of E_{io} applied.

(3) Similarly to the liquid-state counterpart, our solid-state electrolytic capacitor can also be destroyed easily when it is biased in reverse polarity, with aluminum acting the cathode.

References

1. A. DOI, "Handbook of Advanced Electronic and Photonic Materials and Devices," Vol. 5, edited by H. S. Nalwa (Academic Press, New York, 2000) p.1.
2. *Idem.*, *Solid St. Ionics* **147** (2002) 61.
3. *Idem.*, *Phys. Chem. Glasses* **43** (2002) 199.
4. M. MANGION and G. P. JOHARI, *Phil. Mag.* **B 57** (1988) 121.
5. R. VILA, M. GONZALEZ, J. MOLLA and A. IBARRA, *J. Nucl. Mater.* **253** (1998) 141.

Received 25 September 2002

and accepted 20 May 2003